Genuine Pyrimidine Radical Cations Generated by Radiation-Induced Electron Transfer to Butyl Chloride or Acetone Parent Ions

R. Lomoth,[†] S. Naumov,[‡] and O. Brede*,[†]

University of Leipzig, Interdisciplinary Group for Time-Resolved Spectroscopy and Institute of Surface Modification, Permoserstrasse 15, D-04303 Leipzig, Germany

Received: July 10, 1998; In Final Form: December 18, 1998

Radical cations of multiple methylated uracils and thymines were generated by electron transfer to parent ions of solvents of low polarity such as *n*-butyl chloride and acetone. Pulse radiolysis resulted in the transient optical absorption spectra of the pyrimidine radical cations ($Py^{\bullet+}$) which exhibit bands generally peaking around $\lambda = 400$ nm and in acetone showing an additional band in the range of $\lambda_{max} = 500-560$ nm. The identification of the solute radical cations is based on the direct observation of the formation of $Py^{\bullet+}$ by electron transfer ($k = (1-2) \times 10^{10}$ $M^{-1}s^{-1}$), the nucleophilic reaction with the counterion (e.g., Cl^-), the relatively low reactivity with oxygen even for the fully methylated nitrogen groups ($k < 2 \times 10^8$ $M^{-1}s^{-1}$), and the observation of a subsequent electron transfer from triphenylamine to the pyrimidine radical cations proceeding in a diffusion-controlled manner. The solvent dependence of the spectral shape of $Py^{\bullet+}$ was also studied in acetone/*n*-butyl chloride mixtures and was found to depend on the polarity of the surroundings. This phenomenon is explained in terms of a lactam−lactim-like tautomerism of the transient involving the whole plane molecule. Quantum chemical calculations support the experimental findings by explaining the spectral structure and enable the formulation of the lactims as either 1,4- or 3,4-localized.

Introduction

The ionization of deoxyribonucleic acid (DNA) generates, in particular, radical damage in its base unit.[1,2] This can proceed by a UV photolysis[3]or radiolysis[4] effect as well as by one-electron oxidation with oxidizing radicals[5] or in the course of a triplet-sensitized electron-transfer reaction.[6] Radical cations of the pyrimidine and purine bases are the primary products of these oxidation procedures. Hence, much effort has been invested over the past 2 decades into verifying the DNA base radical cations, as was reported in a recent minireview.[2]

Under kinetic conditions, i.e., pulse radiolysis and laser photolysis of solutions of pyrimidines (Py) and purines with real-time optical (absorption) spectroscopy detection, transients were observed which, although described as radical cations, were actually of a radical nature only. This is accounted for by the very rapid conversion of the postulated radical cations via deprotonation or nucleophilic reaction to form radical products, which takes place in times faster than are experimentally observable.[5]

$$\text{Py–e} \longrightarrow [\text{Py}^{\bullet+}] \xrightarrow{^+H_2O} \begin{cases} \text{Py}^{\bullet} + H_3O^+ \\ \text{PyOH}^{\bullet} + H^+ \end{cases} \quad (1)$$

Only in a few cases such as the low-temperature radiolysis of pyrimidines in Freon glasses and detection with EPR[7] could radical cation structures be made probable. Because of the low solubility and the particularly high deprotonation tendency of the natural base units uracil and thymine, methylated derivatives of these compounds were used for the ionization experiments.[5] The identification of the observed ionization products as radical cations is doubtful in this case too and has remained a matter of controversy. Because of their less characteristic spectra, the identification of the pyrimidine transients is indeed very difficult.

In nonpolar solution, the radiation-induced electron transfer from solutes to the parent solvent radical cations is a clear, useful way to generate solute radical cations.[8,9] We decided to also apply this method to the ionization of differently methylated pyrimidines and chose as solvents *n*-butyl chloride[10] (eq 2) and acetone[11] (eq 3), which have gas-phase ionization potentials of 10.7 and 9.7 eV, respectively.[12] For solubility reasons, neither purines nor their methylated derivatives were included in the study. *n*-Butyl chloride radiolysis tends to yield its radical cations and to a lesser extent butene radical cation, which is known to be less reactive in electron-transfer reactions.[10]

$$n\text{-}C_4H_9Cl \rightarrow n\text{-}C_4H_9Cl^{\bullet+},\ C_4H_8^{\bullet+},\ HCl,\ Cl^-,\ C_4H_9^{\bullet},\ \text{etc.} \quad (2a)$$

$$n\text{-}C_4H_9Cl^{\bullet+} + Py \rightarrow Py^{\bullet+} + n\text{-}C_4H_9Cl \quad (2b)$$

Acetone has been used for ionization studies less frequently. To our knowledge, with a dielectric constant of $\epsilon = 20.7$,[12] it is an almost polar solvent that is applicable to radiation-induced electron transfer. In acetone radiolysis, the ionic products formed are a nonlocalized cationic structure and the well-defined acetone anion. The byproducts are the acetone triplet and a number of radicals. The acetone radical cation reacts with solutes in a manner analogous to that of butyl chloride.

$$CH_3COCH_3 \rightarrow CH_3COCH_3]^{\bullet+},\ CH_3C^{\bullet}O^-CH_3,\ CH_3COCH_3{}^{T1},\ \text{etc.} \quad (3a)$$

$$CH_3COCH_3]^{\bullet+} + Py \rightarrow Py^{\bullet+} + CH_3COCH_3 \quad (3b)$$

* Corresponding author.
[†] Interdisciplinary Group for Time-Resolved Spectroscopy.
[‡] Institute of Surface Modification.

10.1021/jp9829804 CCC: $18.00
Published on Web 03/23/1999

Depending on their methyl substitution pattern, the ionization potentials of the pyrimidines are in the range of $I_g = 8-9$ eV. With an ionization potential difference of more than 0.5 eV, under nonprotic and nonpolar conditions pyrimidine radical cations could be formed in accordance with reactions 2b or 3b. Because of the absence of reaction partners (cf. eq 1), under such circumstances these cations ought to be relatively stable. This paper concentrates on the electron-transfer experiments (2b, 3b) from butyl chloride and acetone radical cations to various different pyrimidines performed by pulse radiolysis.

Experimental Section

Chemicals. The following methylation patterns of the basic uracil or thymine structure were used for the experiments.

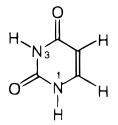

uracil
2,4(1*H*,3*H*)-pyrimidindione

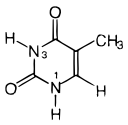

thymine
5-methyl-2,4(1*H*,3*H*)-pyrimidindione

Compound	Abbreviation	Quality
1-methyluracil	1-MU	Chemical Dynamics, Chemalog
3-methyluracil	3-MU	Fluka, >99%
1,3-dimethyluracil	1,3-DMU	Fluka, >99%
1,3,6-trimethyluracil	1,3,6-TMU	*
1-methylthymine	1-MT	Sigma
1,3-dimethylthymine	1,3-DMT	*
3,6-dimethylthymine	3,6-DMT	*
1,3,6-trimethylthymine	1,3,6-TMT	*

* Compounds are not commercially available and were donated by S. Steenken.

n-Butyl chloride (chromatography grade, Aldrich) was dried by A4 molecular sieves. Acetone (spectroscopy grade, Merck) was used as obtained. Triphenylamine (Laborchemie Apolda) was twice recrystallized from *n*-hexane.

Pulse Radiolysis. Experiments were performed with an ELIT pulse transformer type accelerator (Novosibirsk Institute of Nuclear Physics, Russia) delivering 1 MeV, 16 ns electron pulses with a dose of between 50 and 200 Gy. 100 Gy was used as the standard dose per pulse. The optical detection system consisted of a pulsed 900 W xenon lamp (XBO 900, Osram), a Spectra Pro-500 monochromator (Acton Research Corp.), an R4220 photomultiplier (Hamamatsu) or a FND-100Q silicon photodiode (Laser Components), and a TDS 640 500 MHz digitizing oscilloscope (Tektronix).

The samples were bubbled with purest grade nitrogen or oxygen. The experiments were done at 293 K. More details are contained in ref 13.

Quantum-Chemical Methods Used. Today's semiempirical methods such as AM1[14] and PM3[15] can be applied with reasonable accuracy to open-shell systems.[16] We used PM3 for the systematic treating of the pyrimidine radical cations and compared the results with those of AM1 calculations. Geometries, dipole moments, sets of molecular orbitals, and Mulliken population-derived atomic charges for the parent molecules and their radical cations were calculated with HyperChem 5.01 for Windows. The geometry optimizations of all molecules in a vacuum were performed with the Polac−Ribiere conjugate gradient method and direct inversion in the iterative subspace (DIIS) for the better convergence of SCF calculations of the electronic structure. The restricted Hartree−Fock (RHF) approximation was used for the parent molecules. Geometry optimization of the doublet state of the radical cations was carried out using the unrestricted Hartree−Fock (UHF) level.

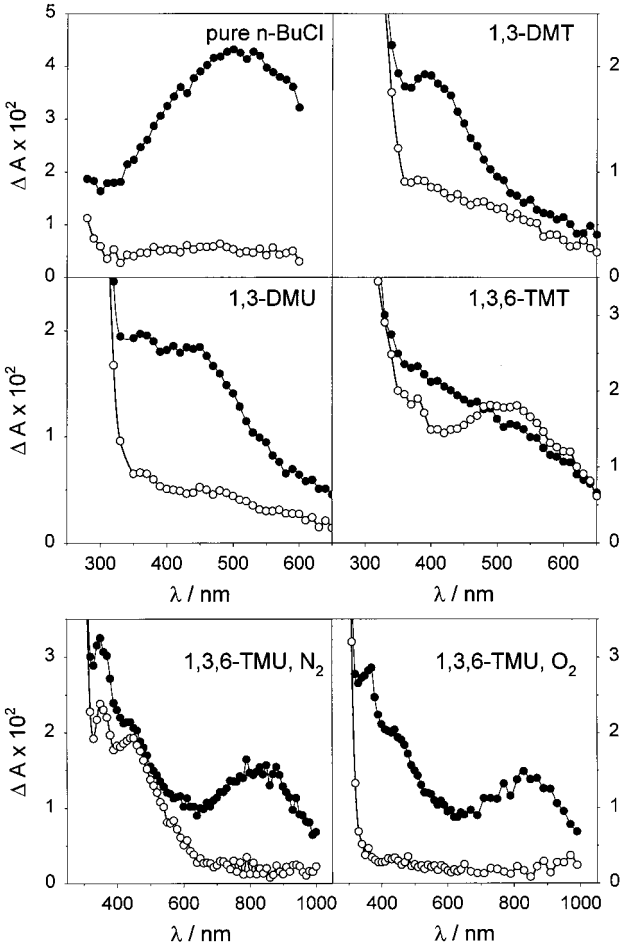

Figure 1. Transient optical absorption spectra taken from pure *n*-butyl chloride ((●) immediately and (○) 300 ns after the electron pulse), from N_2 bubbled 10^{-2} M solutions of various pyrimidines in *n*-butyl chloride ((●) immediately and (○) 1.7 μs after the pulse). The lower part of the figure compares transient spectra of 1,3,6-TMT in N_2-purged and in O_2-saturated solution.

Results and Discussion

As is usual in the literature, we distinguish between uracil and thymine derivatives in order to take into account the immanent influence of the methyl group in the 5-position. The higher methylated pyrimidines are more soluble in both solvents used. For this reason, only part of the more soluble substances could be studied in *n*-butyl chloride.

Pulse Radiolysis of Pyrimidines in *n*-Butyl Chloride Solution. In the pulse radiolysis of pure *n*-butyl chloride (BuCl), a marked optical absorption signal peaking at $\lambda = 500$ nm of the parent radical cation is observed (cf. Figure 1). Assuming first-order kinetics, the lifetime of this species amounts to 90 ns. As the concentrations of the pyrimidines increase ($>10^{-3}$ M), the BuCl time profile is shortened in the sense of a pseudo-first-order reaction and optical absorptions of pyrimidine species appear. This kinetic effect is shown for 1,3-DMU as the solute (Figure 2). The rate constant for the observed electron transfer was determined for all pyrimidines studied to be $k_{2b} = 2 \times 10^{10}$ M^{-1} s^{-1}, i.e., diffusion-controlled with a small residual influence of the primary inhomogeneous distribution of n-$C_4H_9Cl^{\bullet+}$. Hence, for 10^{-2} M Py solution, after a few nanoseconds

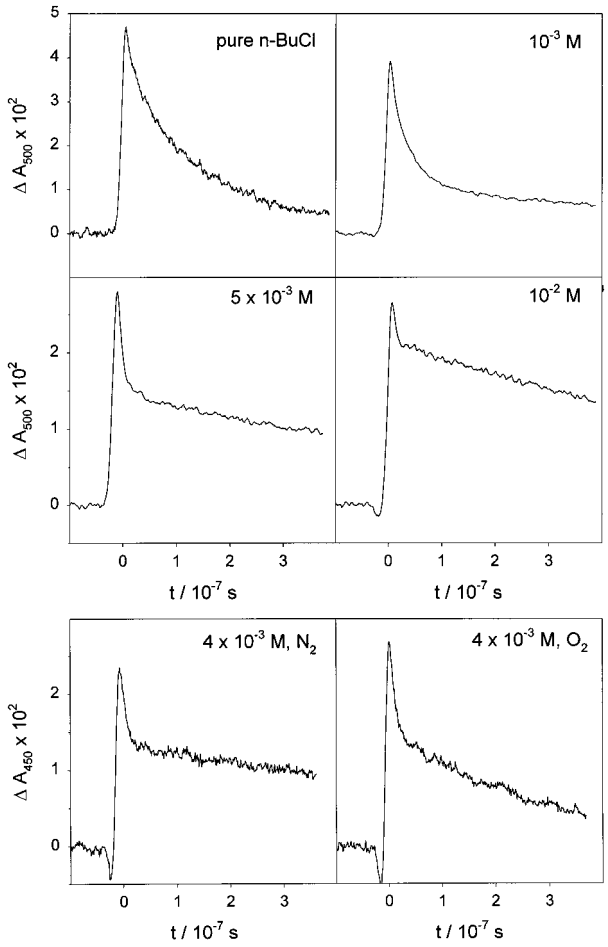

Figure 2. Transient time profiles taken at $\lambda = 500$ nm in the pulse radiolysis of pure *n*-butyl chloride and in deaerated solutions containing increasing concentrations of 1,3-DMU. In the lower part, nitrogen- and oxygen-bubbled samples are compared.

the optical absorption spectra are governed by the Py species, proposed to be $Py^{\bullet+}$ formed in accordance with eq 2a.

Figure 1 gives the absorption spectra of some methylated pyrimidines. The Py species primarily formed show absorption bands ranging from 350 to 550 nm with maxima between 390 and 450 nm. The decay of these species proceeds for all Py under standard dose conditions nearly uniformly with a first half-life time of about 500 ns. The dose per pulse variation indicated a second-order reaction, i.e., a neutralization reaction with the countercharge Cl^- (4), which can also be considered as a reaction with a nucleophile. The products are assumed to be chlorine-substituted pyrimidine radicals, which were not structurally identified in detail.

$$Py^{\bullet+} + Cl^- \rightarrow PyCl^{\bullet} \qquad (4)$$

These products can partially be seen in the absorption spectra, given in Figure 1, as absorptions taken 1.7 μs after the pulse. In the presence of oxygen (10^{-2} M), the pyrimidine radicals were found to disappear rapidly (reaction 5), whereas the precursor $Py^{\bullet+}$ kinetics shows only minor influence (6) as already earlier reported for other radical cations.[17]

$$PyCl^{\bullet} + O_2 \rightarrow \text{products}, \quad k_5 = 2 \times 10^9\ M^{-1}\ s^{-1} \qquad (5)$$

$$Py^{\bullet+} + O_2 \rightarrow \text{products}, \quad k_6 \approx 10^8\ M^{-1}\ s^{-1} \qquad (6)$$

Hence, the identification of the pyrimidine radical cations is

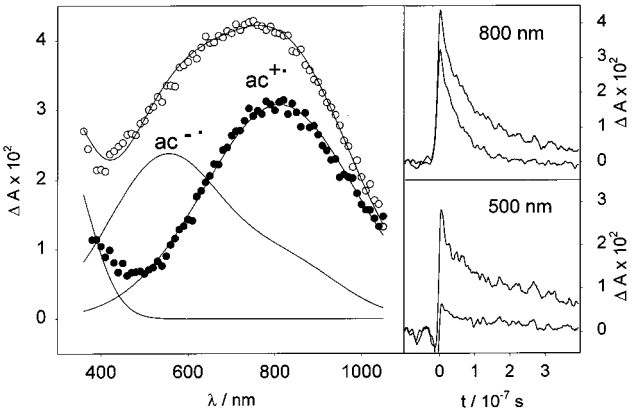

Figure 3. Optical absorption spectra taken in the pulse radiolysis of pure N_2-bubbled acetone (○) and in a sample containing 0.5 M nitromethane (●) immediately after the electron pulse. The solid line gives the difference spectrum between those of (○) and (●) corresponding to the acetone anion absorption. The insets show time profiles taken at 500 and 800 nm in pure acetone (upper profiles) and in the nitromethane-containing solution (lower profiles).

based on the following arguments: (i) formation via electron transfer (2b), (ii) deactivation by neutralization (4) under radical formation, and (iii) less sensitivity vs oxygen than C-centered radicals. Further reactivity arguments are given later.

Pulse Radiolysis of Pyrimidines in Acetone Solution. In acetone, the electron is internally scavenged by the solvent itself (reaction 3a). To transform the electron to a more stable trap and to remove the intense visible absorption of the acetone anion, we used high concentrations (0.5 M) of nitromethane (reaction 7).

$$CH_3C^{\bullet}O^-CH_3 + CH_3NO_2 \rightarrow CH_3COCH_3 + CH_3NO_2^{\bullet-} \qquad (7)$$

This selection is demonstrated in Figure 3, which shows clearly the cation and anion absorption bands of acetone peaking around 820 and 570 nm, respectively. In the presence of the pyrimidines, a clear reduction of the lifetime of the acetone radical cation (inset in Figure 3) is observed. From this, the general reaction rate constant of the charge transfer (3b) from the acetone radical cation to the pyrimidines was determined to be $k_{3b} = 1 \times 10^{10}\ M^{-1}\ s^{-1}$.

Optical absorption spectra of the transient products generated in reaction 3b from the methylated pyrimidines are shown in Figure 4. They show slightly different shapes for the uracil (left column) and thymine species (on the right), which are suggested to be radical cations. The uracil-type radical cations exhibit two absorption bands with maxima around 400 and 550 nm, the latter one being the more intense. By contrast, the thymine-type radicals have bands around 380 nm and less pronounced ones at 500 nm (see right-hand column in Figure 4). The first half lifetimes of the species under standard dose conditions are uniformly about 500 ns throughout the whole spectrum, apart from the contribution of a little radical tail at the UV border. The effect of oxygen is the same as that observed in butyl chloride (reaction 6) and can thus be neglected for our purposes. For the identification of the primary Py transients as radical cations, the same criteria hold as listed above for butyl chloride as the solvent.

Tautomerism of the Pyrimidine Radical Cations. When comparing the spectra of the Py radical cations detected in both solvents, a marked difference in shape emerges, particularly for the uracils, for which in acetone a second band appears peaking around 500−550 nm. This band exhibits the same kinetics as

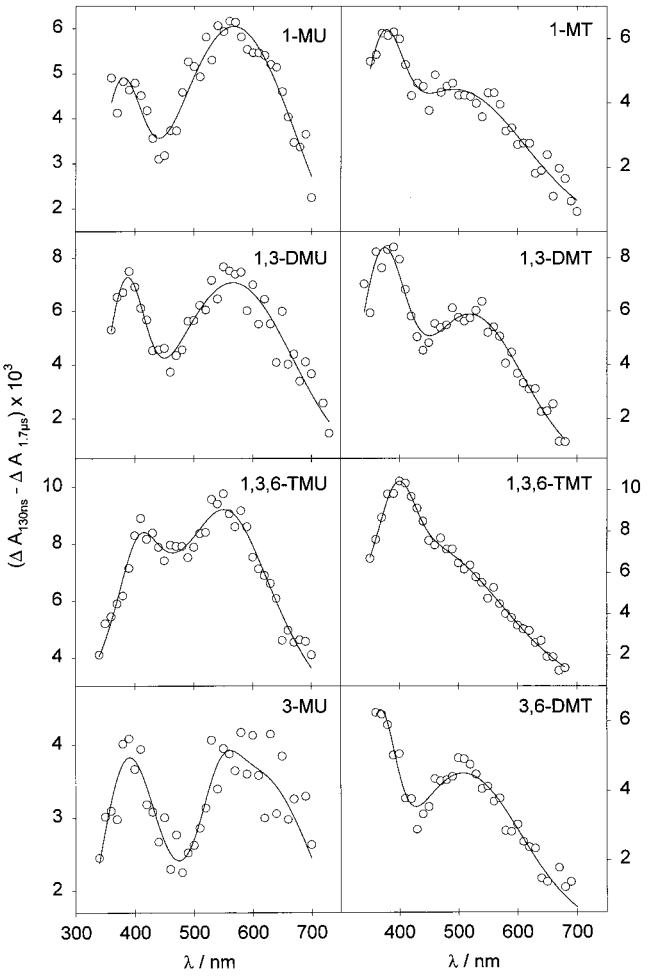

Figure 4. Spectra of pyrimidine radical cations taken in the pulse radiolysis of 10^{-2} M solutions of various Py in O_2-bubbled acetone solution containing 0.5 M nitromethane, immediately after the pulse. (Spectra have been corrected for the long-lived acetone transients absorbing at $\lambda < 400$ nm by subtracting spectra taken at 1.7 μs.)

that at 400 nm. In our search for experimental evidence to explain this phenomenon, we used various mixtures of butyl chloride and acetone as solvents and a constant scavenger concentration. At low acetone concentration under these conditions, a charge transfer from the butyl chloride radical cation to the acetone initially takes place (8) due to the difference in the ionization potentials of these solvents (see above).

$$n\text{-}C_4H_9Cl^{\bullet+} + CH_3COCH_3 \rightarrow n\text{-}C_4H_9Cl + CH_3COCH_3]^{\bullet+} \quad (8)$$

Subsequently, transfer (3b) occurs, resulting in the pyrimidine radical cations. At higher acetone concentrations, the direct formation of acetone radical cations also takes place, whereas the anionic part is eliminated in each case by the dissociative electron capture of butyl chloride. These experiments are demonstrated in Figure 5, which shows spectra taken after 15 ns for a 10^{-2} M solution of 1,3-dimethyluracil in butyl chloride admixed with molar concentrations of acetone. Two effects can be observed: (i) the radical cation yield rises with increasing acetone concentration, which is explained by the slightly higher free ion yield in this solvent; (ii) the spectral shape changes gradually with increasing amounts of acetone. This effect on the spectral shape is nonlinear with respect to the molecular abundance of acetone as shown in the inset of Figure 5, where

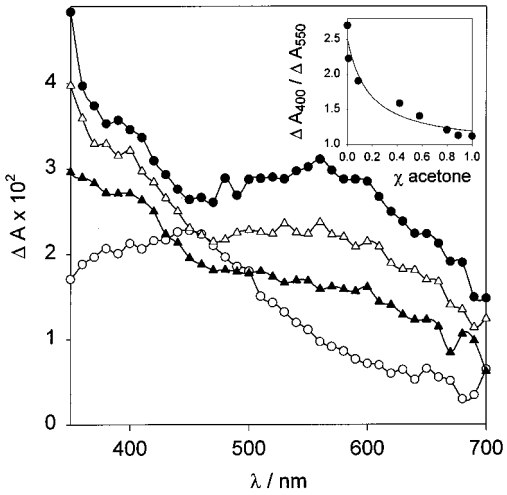

Figure 5. Transient absorption spectra taken in the pulse radiolysis of solutions of 1,3-DMU in a solvent mixture of *n*-butyl chloride and acetone of different composition. The inset shows the plot of the ratio between the 400 and 550 nm absorptions vs the composition of the solvent mixture (○) pure BuCl, (▲) 5 M acetone (35%), (△) 7 M acetone (50%), (●) pure acetone).

the ratio between the 400 nm and the 550 nm absorptions is plotted against the consistency of the mixture.

We try to explain this behavior in terms of the change of the polarity of the sample, i.e., by the change of the dielectric properties of the mixture of a component of a low (butyl chloride, $\epsilon = 7.4$) and a higher dielectric constant (acetone, $\epsilon = 20.4$). Hence, the surrounding solvation shell of the solute is changed and a structural tautomerism can occur. When considering the structure of the pyrimidine molecules, a number of tautomeric forms can be imagined. In this connection, any tautomerism of the pyrimidine parent molecules could be excluded by H NMR measurements in a variety of solvents.

Hence, we interpret the experimental observation of the different optical absorption behavior of the radical cations of the pyrimidines generated by electron transfer in two differently polar solvents as a transient tautomerism in lactam−lactim-like forms.

Because the effect of the solvent polarity on the transient spectra was even observed with pyrimidines methylated on both N-atoms, we had to assume a tautomerism involving protons of the methyl groups. Possible tautomeric structures resulting from the lactam structure (II) are a 1,2- and a 3,4-lactim (I, III) as shown in eq 9.

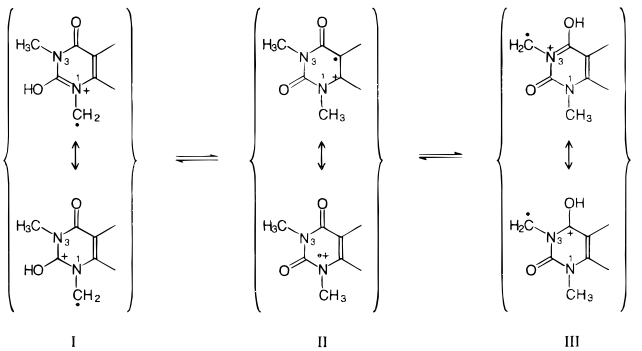

(9)

The structure and equilibrial position of the tautomeric forms certainly ought to be governed by the methylation pattern. Table 1 gives a survey of the experimentally investigated cases.

TABLE 1: Comparison of Calculated Vertical Excitation Energies (nm) and of the Experimentally Obtained Absorption Maxima of the Radical Cations of Lactam (in Butyl Chloride) and Lactim Structures[a]

	lactam			lactim		
pyrimidine	λ_{exp}, BuCl (nm)	λ_{calc}, (nm) PM3	λ_{calc}, (nm) AM1	λ_{exp}(max), acetone (nm)	λ_{calc}, (nm) PM3	λ_{calc}, (nm) AM1
1-MU	*b*	374 (1.00)	366 (1.00)	380	410 (1.00)	389 (1.00)
		692 (0.09)	485 (0.06)	570	468 (0.55)	453 (0.64)
					876 (0.83)	813 (0.76)
3-MU	*b*	375 (1.00)	366 (1.00)	390	417 (0.17)	394 (0.17)
		777 (0.08)	572 (0.11)	560	523 (0.42)	529 (0.22)
					790 (1.00)	798 (1.00)
1,3-DMU	400	372 (1.00)	371 (1.00)	390	432 (0.13)	401 (0.14)
		764 (0.08)	566 (0.08)	560	525 (0.56)	498 (0.32)
					803 (1.00)	783 (1.00)
1,3,6-TMU	380	383 (1.00)	370 (1.00)	410	437 (0.13)	403 (0.49)
	820	713 (0.07)	533 (0.09)	550	508 (0.56)	483 (0.57)
					789 (1.00)	769 (1.00)
1-MT	*b*	420 (1.00)	394 (1.00)	380	433 (1.00)	415 (1.00)
		589 (0.03)	441 (0.08)	500	480 (0.65)	463 (0.81)
					897 (0.62)	828 (0.90)
1,3-DMT	400	408 (1.00)	408 (1.00)	380	367 (1.00)	342 (1.00)
		647 (0.04)	495 (0.01)	520	531 (0.56)	518 (0.35)
					810 (0.49)	778 (0.90)
3,6-DMT	*b*	414 (1.00)	406 (1.00)	370	364 (1.00)	344 (0.90)
		619 (0.05)	477 (0.02)	500	538 (0.43)	510 (0.50)
					807 (0.58)	784 (1.00)
1,3,6-TMT	400	417 (1.00)	408 (1.00)	400	368 (1.00)	352 (1.00)
		615 (0.04)	473 (0.01)	530	540 (0.39)	508 (0.52)
					802 (0.51)	771 (0.36)

[a] Relative oscillator strength given in parentheses. [b] No values due to insufficient solubility of Py.

Because we did not see any chance of further experimental proof of the hypothesis of transient tautomerism of the pyrimidine radical cations, we performed semiempirical quantum chemical calculations for spectra and structure interpretation.

Quantum Chemical Calculation of Lactam−Lactim Radical Cation Structures and of the Corresponding Transient Spectra. Certainly, the validity of simple semiempiric open-shell quantum chemical programs for heterocyclic systems is limited. Nevertheless, we made such calculations for getting a feeling for favored transient structures and transient optical absorption spectra.

Using the aforementioned program, we first minimized the binding energies of all possible lactim-like radical cation structures, as demonstrated in Figure 7 for the examples of 1-MU, 3-MU, and 1-MT. The differences in binding energies compared to the lactam structure (calculated with PM3 and AM1) are given below the formula structures. These tautomers of lowest energy (compared to the lactam) were used for the spectra calculations of the transients. These structures for all of the studied pyrimidines are given in Figure 8. The most stable tautomers were found to be 5−12 kcal mol^{-1} more stable compared to the lactam and 6−18 kcal mol^{-1} more stable compared to the tautomers of least stability. In the case of tautomeric structures exhibiting comparable binding energy, we favored for spectra calculation those structures involving the *N*-methyl group. In any case, most of the possible tautomeric structures could be ruled out differing by more than 4−5 kcal mol^{-1} from the most favored structure. Surprisingly, a structure we tentatively assumed to be one of the more reasonable tautomers (structure I in eq 9) is less stable than the structures obtained after proton shift between the substituents at N(3) and C(4) (Figure 7, 3-MU) as well as between positions N(1) and C(4) (Figure 7, 1-MU and 1-MT). Furthermore, it was found that even with compounds with hydrogen atoms directly connected to N(1) or N(3), the lactim structures with the highest stabilization energy are those resulting from the shift of an methyl proton (cf. Figure 7).

In detail, the calculations of the spectra were performed as follows. Electronic transition energies were calculated with single excited configuration interaction with restricted open-shell (ROHF) option, whereas structures for $Py^{\bullet+}$ were calculated with UHF. This approach was adopted because the configuration interaction (CI) method for the calculation of the UV−vis electronic spectra of systems with an unpaired electron is only available for ROHF.

It was found that the two highest double occupied, the single occupied (SOMO), and the three lowest unoccupied MOs play a preponderant role in the description of the electronic transitions studied. We therefore used CI involving five electrons distributed over six CI-active MOs. Furthermore, it is postulated that the gas-phase radical cation spectra are quite similar to those in the liquid state.

Analysis of the MOs shows that the lowest energy transitions have to be assigned to $\pi \rightarrow \pi^*$ transitions. The calculations yielded different spectra for the lactam and the lactim tautomeric forms. The results of the calculations compared with the experimental data are given in Table 1.

For the lactam radical cation, excitation from SOMO to LUMO appearing between $\lambda = 372$ and 417 nm has a very high oscillator strength for all pyrimidines, which excellently corresponds to the measured data. Excitation from the highest double occupied MO to SOMO yields a band in the IR spectral range exhibiting a weak oscillator strength, which could explain an experimental absorption band observed for the radical cation of 1,3,6-TMU with λ_{max} around 820 nm.

The eigenvalues of the MOs of the lactim radical cation sharply differ from those of the lactam. Excitation from SOMO to LUMO exhibits the smallest energy for all pyrimidine radical cations. The next two transitions are either those of the excitation of the electron from the highest double occupied π-MO to SOMO or those from SOMO to the third unoccupied π-MO, which depends on the energy difference of these orbitals. The excitation from SOMO to the second unoccupied σ^*-MO is

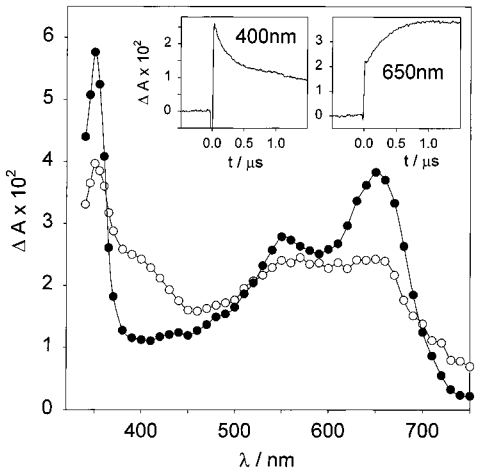

Figure 6. Transient optical absorption spectra taken in the pulse radiolysis of a solution of 10^{-2} M 1,3-DMU and 5×10^{-5} M triphenylamine in nitrogen-purged acetone containing 0.5 M nitromethane as electron scavenger. (○) shows the spectrum immediately after the pulse caused by the $Py^{\bullet+}$ absorption, whereas (●) gives predominantly the $TPA^{\bullet+}$ spectrum taken after 1 μs. The insets show time profiles at 400 nm mainly describing the decay of $Py^{\bullet+}$ and at 650 nm showing the formation of $TPA^{\bullet+}$.

symmetry forbidden as a $\pi \rightarrow \sigma^*$ transition and therefore exhibits only limited oscillator strength.

The calculations reproduce the observed spectra with reasonable accuracy (cf. Table 1) and support the assignment of the experimentally observed additional vis band to the lactim form of the pyrimidine radical cations. For the third electronic transition of the lactim resulting from the calculations we have not found experimental evidence. A possible explanation for this might be that energy differences are small in this range of a wavelength scale. Therefore, this band might be shifted considerably to the infrared due to the error of the calculated energies.

The interpretation of the lactam−lactim tautomerism of the $Py^{\bullet+}$ can be based on considerations about the influence of the higher polarity of acetone, in comparison to butyl chloride. Another variant could be the direct involvement of acetone in the proton transfer mechanism. We investigated this problem also by quantum chemistry. Hence, we undertook semiempiric calculations (PM3, AM1) of a molecular aggregate of the lactam radical cation with one or two acetone molecules. It resulted that, in the case of the acetone mediated proton transfer, the binding energy difference between the starting and the final state (formally an aggregate between acetone enol and the lactime radical cation) amounts to about -3 kcal mol^{-1} for one and $+8$ kcal mol^{-1} for two acetone molecules; i.e., this solvent mediated process is unfavorable in comparison to the intramolecular proton transfer described above.

Charge Transfer from the Pyrimidine Radicals to Triphenylamine. The stepwise charge transfer from the solvent parent ion to the pyrimidines and subsequently to a further scavenger with known radical cation properties seems to be a very convincing argument for intermediate radical cation identification. Hence, we realized such a reaction sequence using triphenylamine as the final charge trap (reaction sequence 10). The experiments were performed in both butyl chloride and acetone and are demonstrated here for the latter case.

$$CH_3COCH_3]^{\bullet+} + Py \rightarrow Py^{\bullet+} + CH_3COCH_3;$$
$$Py^{\bullet+} + Ph_3N \rightarrow Ph_3N^{\bullet+} + Py \quad (10)$$

As an example, Figure 6 shows for the case of 1,3-dimethyluracil the $Py^{\bullet+}$ first formed (20 ns after the pulse), which is subsequently transformed to $Ph_3N^{\bullet+}$ in accordance with sequence (10). In this case, only a very small triphenylamine concentration of 5×10^{-5} M was used. The time profiles given as insets show the kinetic relation of pyrimidine cation decay (400 nm) and triphenylamine radical cation formation (650 nm). This behavior has been studied for several pyrimidines, including variation of the triphenylamine concentration, as previously described.[18]

In the nonpolar solvents used and for the methylated pyrimidines, the charge-transfer sequence (10) verifies the identification of the pyrimidine transients observed as radical cations. In aqueous solution, the situation is much more complicated. In a forthcoming paper, we will report on the identification of pyrimidine species in aqueous medium based on the evaluation of the kinetics of subsequent product formation.

Analysis of the Extinction Coefficients of the Pyrimidine Lactame and Lactim Radical Cations. The analysis of the optical properties of the absorption bands observed was attempted in two different ways: (i) by calculating the transient extinction coefficients by determining the absorbed dose and recalculating the transient concentration and (ii) by comparison with an internal standard with known extinction properties. The first method suffers from the uncertainty of the comparability of the ion yields of the scavenger ions in view of the different scavenging capabilities (which determines the position in the scavenger curve[19]). Hence, this method was only used for a rough estimate of extinction coefficients, yielding values of about $\epsilon_{\cong 400nm} = 8000$ M^{-1} cm^{-1} for the band of the lactam radical cations in BuCl and $\epsilon_{\cong 400,550nm} = 3000$ M^{-1} cm^{-1} for both lactim radical cation bands found in acetone.

The second method uses an internal standard involved in the reaction mechanism via the stepwise charge transfer from the parent solvent ion to the pyrimidine and from its cation to a second scavenger with well-known radical cation properties, as described above,[18] reaction sequence 10. For this purpose, triphenylamine ($TPA^{\bullet+}$, $\epsilon_{650nm} = 29000$ M^{-1} s^{-1}, refs 20 and 21) was employed. Considering a formation efficiency of the standard cations of 60% for the example of $c_{TPA} = 5 \times 10^{-4}$ M, a more exact extinction coefficient was determined as shown in Table 2 for both the lactam and the lactim forms of $Py^{\bullet+}$. These values do not contradict those estimated with method (i) and demonstrate that the internal standard method (ii) is the only acceptable one for nonpolar systems.

Each radical cation type (i.e., the lactam and the lactim forms) differs in its electronic structure, and put simply, the lactam form represents the radical cation with allyl mesomery between the N1 amine group and the olefinic bond between C5 and C6, whereas the lactim looks more like a distonic radical cation. This seems to be the reason for the different optical absorption spectra and also for the different extinction coefficients of both species types.

Furthermore, it should be stated that the extinction coefficients of all the pyrimidine radical cations studied in this paper have between 4 and over 10 times higher extinction coefficients than those found for the species formed in aqueous solution, also ascribed to be pyrimidine radical cations.[5] Spectral analysis of this species also yields slight distinctions, and in view of this and the enormous difference in the extinction coefficients, the cationic nature of the species in aqueous solution seems to be questionable.

TABLE 2: Extinction Coefficients of the Pyrimidine Radical Cations in the Lactam (BuCl) as well as Lactim Form (Acetone), Determined with Triphenylamine Radical Cation as an Internal Standard

	BuCl		acetone	
pyrimidine	λ_{max}/nm	ϵ/dm^3 mol^{-1} cm^{-1}	λ_{max}/nm	ϵ/dm^3 mol^{-1} cm^{-1}
1-MU	*a*		380	3300
			570	4100
3-MU	*a*		390	2600
			560	2600
1,3-DMU	400	13000	390	6600
			560	6600
1,3,6-TMU	380	22000	410	5700
	820	11000	550	6200
1-MT	*a*		380	4300
			500	3000
1,3-DMT	400	13000	380	5700
			520	4000
3,6-DMT	*a*		370	4500
			500	3200
1,3,6-TMT	400	15000	400	5700
			500	3600

[a] No values due to insufficient solubility of Py.

Structure and Kinetics of the Pyrimidine Radical Cations. Looking at the pyrimidine skeleton, ionization of the molecules ought to generate radical cations with positive charges delocalized between the N(1) and the olefin group between C(5) and C(6), in the sense of a heteroallyl mesomery. This should generally hold, including the differently methylated Py structures. As a consequence, N(1) and C(5) are the centers of the lowest electron density and C(5) the point favored for nucleophilic attacks. These considerations are well supported by the extensive information in the literature concerning pyrimidine radical transients derived from the radical cations and by quantum chemical calculations.[22] However, owing to the aqueous samples used for the foregoing studies, direct observation and in particular the certain identification of $Py^{\bullet+}$ were not possible.

All in all, in this paper five kinetic and spectroscopic criteria were found to be fulfilled which argue for the direct observation of $Py^{\bullet+}$ in nonpolar solution in the nanosecond time range.

(i) Their generation proceeds via electron transfer from the nucleobases to the solvent parent ions, as was demonstrated for both *n*-butyl chloride and acetone.

(ii) The pyrimidine radical cations decay by reaction with the nucleophile, here with chloride; only in one case (3-methyluracil) was deprotonation to a neutral radical faster than neutralization.

(iii) It was generally found that the pyrimidine radicals are not sensitive to oxygen. This is also known for other radical cation types.

(iv) In the presence of low amounts of an additional scavenger with lower ionization potential (here triphenylamine), the cations $Py^{\bullet+}$ are involved in a further electron transfer (10).

(v) The crucial argument, however, consists of the following observation: the spectral shape of the pyrimidine radical cations is not very characteristic, but different from those of the pyrimidine radicals observed in aqueous solution,[5] whereas the extinction coefficients of $Py^{\bullet+}$ generated in BuCl and acetone are dramatically higher than those of the pyrimidine radicals.

At first sight, the different shape of the pyrimidine cation spectra in *n*-butyl chloride and acetone as solvents seems to call into question the uniform treatment of the transients as radical cations. But both absorption bands (400 and 550 nm) and, more commonly, the whole visible solute transient spectra exhibit uniform kinetic behavior in, for example, reactions 4, 6, and 10. Therefore, we postulate a transient tautomerism caused by the molecular surroundings of $Py^{\bullet+}$ given either by the nonpolar *n*-butyl chloride or acetone which exhibits higher polarity, or mixtures of these solvents. As demonstrated in Figure 5, the addition of the more polar solvent affects the ratio between the tautomeric forms much more than in proportion to the molar ratio. This is concluded from consideration of the inclusion of the added molecules to the solvation environment (shell), which ought to prefer the more polar molecules. Nevertheless, solvation shell formation and exchange in the solvents studied and their mixture is a very dynamic process.[23]

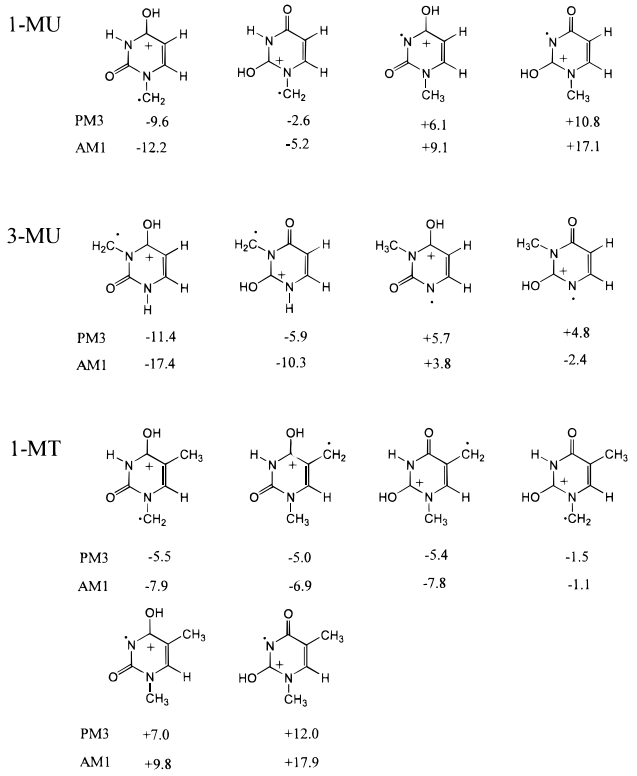

Figure 7. Possible structures of lactim-like tautomers of the radical cations of 1-MU, 3-MU, and 1-MT with the differences in binding energy compared to the lactam structure (calculated with PM3 and AM1).

Transient tautomerism of radical cations was reported for the case of a keto−enol correlation in the case of methyl-substituted aromatic carbonyl compounds[25] such as *o*-vinylbenzaldehyde. A recent review of this field is given in ref 26. As far as we are aware, the transient tautomerism of the lactam−lactim form of radical cations is reported in our paper for the first time.

For the assignment of either the lactam or the lactim structure to the defined solvent (butyl chloride or acetone), we first used an analogy to a similar tautomerism described by Dubois et al.,[24] which stated for the ground state molecules that under more polar conditions the lactim form should dominate, whereas in the nonpolar system the lactam structure should be favored. As this interpretation also seems to be valid for the transient tautomerism of the pyrimidine radical cations, we assigned the lactam form to the butyl chloride medium and the lactim structure to acetone. This interpretation, however, can hold only for aprotic systems that are unable to form hydrogen bonds.

The quantum chemical calculations support this hypothesis. Hence, we were able to calculate optimized transient lactim structures on the basis of calculated binding energies, as shown in Figure 7 for 1-MU, 3-MU, and 1-MT. Neglegting the

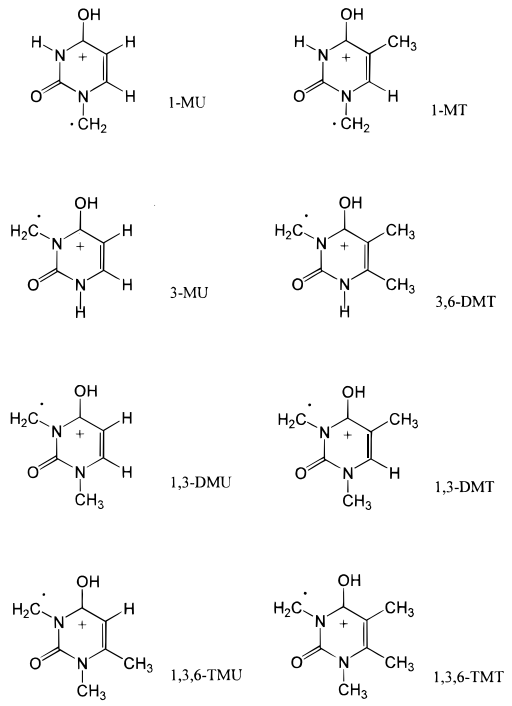

Figure 8. Lactim radical cation structures of the studied pyrimidines optimized for lowest binding energy. For these cases, the spectral transitions were calculated (see Table 1).

structures which do not involve the lone pairs of the N-atoms, the most favored structures of lowest energy (cf. Figure 8) were used for calculating optical absorption spectra which correspond well to the experimental band position and the spectral structure.

The lactim structures varied for the different pyrimidine radical cations between the 1,4-lactim and the 3,4-lactim isomer (cf. Figure 8). For the thymines studied, the 3,4-form seems to dominate with the exception of 1-MT, which for the form of lowest binding energy exhibits separation of spin and charge between the methyl substituent at N1 and the C4 positions. For uracils, both forms (1,4- and 3,4-lactim transient isomer) were obtained. In order not to read too much into these results, it should be generally stated that within the pyrimidine molecule skeleton some tautomeric forms may exist which rapidly rearrange from one form to the other. This would explain the spin-charge separated (distonic radical cation) form mentioned for the cases of 1-MT and 1-MU.

Because of the rapid intramolecular structure exchange between (both) tautomeric forms, chemical reactivity over the whole spectrum appeared to be uniform, as observed in our experiments described above, and in particular for the case of the subsequent electron transfer (10) under the formation of radical cations of a second scavenger.

Conclusions

The charge transfer from solvent parent radical cations to a variety of methylated pyrimidines yields pyrimidine radical cations observable in the nanosecond time range. These radical cations show a transient tautomerism and exist in *n*-butyl chloride in the lactam and in acetone in a lactim-like form. They display kinetic and spectral properties which differ much from pyrimidine species formed in aqueous solution. Hence, the extinction coefficients in the optical absorption maxima are very typical of radical cations and are in the range of 13000−15000 M^{-1} cm^{-1} for the lactam form and 3000−6000 M^{-1} cm^{-1} for the lactim radical cations. Despite frequent claims to this effect in the past, this is the first time that pyrimidine radical cations have been directly detected at room temperature.

References and Notes

(1) von Sonntag, C. *The Chemical Basis of Radiation Biology*; Taylor and Francis: London, 1987.
(2) Steenken, S. *Biol. Chem.* **1997**, *378*, 1293.
(3) Stemp, E. D. A.; Barton, J. K. *Met. Ions Biol. Syst.* **1996**, *33*, 325.
(4) Bernhard, W. A. *Adv. Radiat. Biol.* **1981**, *9*, 199. Steenken, S. *Chem. Rev.* **1989**, *89*, 503. Close, D. M. *Magn. Reson. Rev.* **1991**, *15*, 241. Hüttermann, J. In *Radical Ionic Systems: Properties in Condensed Phases*; Lund, A., Shiotano, M., Eds.; Kluver: Dordrecht, The Netherlands, 1991; p 435. Becker, D.; Sevilla, M. D. *Adv. Radiat. Biol.* **1993**, *17*, 121.
(5) Deeble, D. J.; Schuchmann, M. N.; Steenken, S.; von Sonntag, C. *J. Phys. Chem.* **1990**, *94*, 8186.
(6) Geimer, J.; Brede, O.; Beckert, D. *Chem. Phys. Lett.* **1997**, *276*, 411. Wood, P. D.; Redmond, R.W. *J. Am. Chem. Soc.* **1996**, *118*, 4256.
(7) Rhodes, C. J.; Podmore, I. D.; Symons, M. C. R. *J. Chem. Res. Synop.* **1988**, 120.
(8) Brede, O.; Mehnert, R.; Naumann, W. *Chem. Phys.* **1987**, *115*, 279.
(9) Mehnert, R.; Brede, O.; Naumann, W. *J. Radiolanal. Nucl. Chem.* **1986**, *101*, 307.
(10) Arai, S.; Kira, A.; Imamura, M. *J. Phys. Chem.* **1976**, *80*, 1968. Mehnert, R.; Brede, O.; Naumann, W. *Ber. Bunsen-Ges. Phys. Chem.* **1982**, *86*, 525.
(11) Rodgers, M. A. J. *Trans. Faraday Soc.* **1971**, *67*, 1029. Rodgers, M. A. J. *J. Chem. Soc., Faraday Trans. 1* **1972**, *68*, 1278. Robins, A. J. *J. Chem. Soc., Faraday Trans. 1* **1973**, *69*, 2036.
(12) Lide, D. R., Ed. *Handbook of Chemistry and Physics*, 73rd ed.; CRC Press: Boca Raton, 1992; p 10−233.
(13) Brede, O.; Orthner, H.; Zubarev, V.; Hermann, R. *J. Phys. Chem.* **1996**, *100*, 7097.
(14) Dewar, M. J. S.; Zoebisch, E. G.; Healy, E. F.; Stewart, J. P. P. *J. Am. Chem. Soc.* **1985**, *107*, 3902.
(15) Stewart, J. P. P. *J. Comput. Chem.* **1989**, *209*, 221; *J. Comput.-Aided Mol. Design* **1990**, *4*, 1.
(16) Schweig, A.; Thiel, W. *J. Am. Chem. Soc.* **1981**, *103*, 1425. Troe, J.; Weizel, K.-M. *J. Chem. Phys.* **1988**, *88*, 7030. Grimme, S. *Comput. Chem.* **1994**, *15*, 425. Grimme, S.; Löhmannsröben, H.-G. *J. Phys. Chem.* **1992**, *96*, 7005. Rodriguez, J.; Scherlis, D.; Estrin, D.; Aramendia, K. P.; Negri, R. M. *J. Chem. Phys. A* **1997**, *101*, 6998. Mora, M. A. *Int. J. Quantum Chem.* **1997**, *65*, 767.
(17) Brede, O.; David, F.; Steenken, S. *J. Chem. Soc., Perkin Trans. 2* **1995**, *2*, 23.
(18) Lomoth, R.; Brede, O. *Chem. Phys. Lett.* **1998**, *288*, 47.
(19) Warman, J. M. In *The Study of Fast Processes and Transient Species by Electron Pulse Radiolysis*; Baxendale, J., Busi, F., Eds.; D. Reidel: Dordrecht, 1982; p 433.
(20) Burrows, H. D.; Greatorex, D.; Kemp, T. J. *J. Phys. Chem.* **1972**, *76*, 20.
(21) Nelson, R. F.; Philip, R. H., Jr. *J. Phys. Chem.* **1979**, *83*, 713.
(22) Colson, A.; Besler, B.; Close, D. M.; Sevilla, M. D. *J. Phys. Chem.* **1992**, *96*, 661. O'Donnell, T. J.; LeBreton, P. R.; Petke, J. D.; Shipman, L. L. *J. Phys. Chem.* **1980**, *84*, 1975. Schuchmann, H.-P.; Deeble, D. J.; Olbrich, G.; von Sonntag, C. *Int. J. Radiat. Biol.* **1987**, *51*, 441.
(23) Kavarnos, G. J. *Fundamentals of Photoinduced Electron Transfer*; VCH Publishers: New York, 1993; pp 322.
(24) Bensaude, O.; Chevrier, M.; Dubois, J. E. *J. Am. Chem. Soc.* **1978**, *100*, 7055. Chevrier, M.; Bensaude, O.; Guillerez, J.; Dubois, J. E. *Tetrahedron Lett.* **1980**, *21*, 3359.
(25) Huben, K.; Zhu, Z.; Bally, T.; Gebicki, J. *J. Am. Chem. Soc.* **1997**, *119*, 2825.
(26) Gebicki, J.; Bally, T. *Acc. Chem. Res.* **1997**, *30*, 477.